Journal of Materials and Engineering Structures

Research Paper

Sustainable Development of High-Volume Fly Ash Self-Compacting Concrete Incorporating Bottom Ash and Recycled Concrete Aggregates

Amardeep Meena [a], Navdeep Singh [a], S.P. Singh [a, *]

[a]Department of Civil Engineering, Dr B R Ambedkar National Institute of Technology, Jalandhar, 144 011, India

ARTICLE INFO

Article history :

Received : 21 July 2023

Revised : 30 September 2023

Accepted : 13 October 2023

Keywords:

High-volume fly ash self-compacting concrete

Coal bottom ash

Mechanical properties

Recycled concrete aggregates

Durability properties

ABSTRACT

Incorporating by-products like coal bottom ash (BA), recycled concrete aggregates (RCA), and fly ash (FYA) in concrete is an essential step toward green and sustainable development in construction sector. For sustainable utilization of RCA as natural coarse aggregates (NCA) and BA as natural fine aggregates (NFA) in high-volume fly ash self-compacting concrete (HVFYA-SCC), this study investigates ten numbers of designed HVFYA-SCC mixes. HVFYA-SCC mixes were developed with varying content of ordinary Portland cement, FYA (60%), NCA, NFA, RCA (maximum 50%) and BA (maximum 30%). The substitution of 20% BA and 25% RCA in HVFYA-SCC mixes increased compressive and split tensile strengths after 120 days of curing, while further substitution (s) led to a drop in properties. Similarly, at 120 days of curing the maximum electrical resistivity was achieved (20% BA and 25% RCA), while all mixes under ultrasonic pulse velocity resulted in the 'good category.' Also, the same mix resulted in lower sorptivity values for maximum curing. A good correlation ($R^2 > 0.8$) was observed among the tested mechanical and durability properties. The outcomes of this study indicate valuable information on the performance and potential benefits of using HVFYA-SCC in advanced structural designs for upcoming concrete industry. Furthermore, the findings successfully support the implementation of designed concretes as sustainable and environmentally-friendly alternative to conventional concrete(s).

1 Introduction

Concrete is vital for transportation infrastructure, such as roads, bridges, airports, and railways; production consumes vast amounts of natural resources [1]. This has prompted the construction sector to focus on creating more environmentally friendly concrete solutions, including recycled concrete. However, the increasing demand for aggregates used in making concrete has put a strain on the environment and natural resources. India ranks as the third major producer of construction waste worldwide, following USA and China [2]. This waste generation ranges between 100 and 400 MT annually [3], with urban cities being the primary contributors. As per the United Nations Department of Economic and Social Affairs [4], it is estimated that 300-400 million individuals will migrate to cities in the forthcoming periods, resulting in a demand for 600-

* *Corresponding author. Tel.: +91 9814088475.*
E-mail address: spsingh@nitj.ac.in

e-ISSN: 2170-127X,

RESEARCH REVIEW of Sciences and Technologies

700 MT of aggregates [5]. However, India is currently facing a shortage of these aggregates, making it imperative for states to focus on urbanization and resource utilization efficiency. To address this issue, efforts have been made to effectively use construction and demolition waste (C&DW) as aggregates in producing new concrete, known as recycled concrete aggregates (RCA). The incorporation of RCA in place of natural coarse aggregates (NCA) has demonstrated significant benefits. For instance, it has led to a 10-times reduction in CO_2 emissions and an 8-times decrease in energy consumption [6].

Furthermore, concrete with 100% RCA as NCA has shown a reduction in global warming potential by approximately 70% [7]. Although RCA exhibits lower mechanical properties related to concrete made with NCA, the quality of the RCA plays a crucial role in determining its suitability for construction applications [5]. However, it is worth noting that an improvement in the mechanical properties of concrete with NCA as RCA is limited to 25% [8-10]. Coal-fired power plants significantly contribute to air pollution, responsible for 96% of total emissions and generating various waste products, including coal bottom ash (BA) and fly ash (FYA). Both wastes have high leaching abilities and can be toxic to the soil [11]. In India, approximately 232 million tons of FYA are produced yearly, with 92% of it being utilized in various industries, such as cement, concrete, highways, and flyovers [12]. BA is also a byproduct of coal-fired thermal power plants, with around 9.7 million tons produced in the United States in 2017 and India and China producing approximately 90 and 30 metric tons, respectively, in recent years. Other countries in Asia, Europe, and America contribute about one-tenth to one-sixth of the worldwide BA generation [13]. With India's growing demand for power, coal-fired thermal power plants will continue to show an important role in meeting energy needs in the coming decades, despite the country's goal of achieving net-zero emissions and becoming carbon neutral by 2070 [14].

Self-compacting concrete (SCC) is a specialized concrete that spread and fill densely reinforced areas while effectively sealing corners of formwork and compacting itself under its own weight. The primary requirements for SCC are filling gaps, flowing effortlessly, and resisting segregation. These properties have been extensively studied and documented [15-19]. As developing countries like India and China experience an increase in infrastructure projects, there is a growing need for the fundamental components of concrete, including cement, natural fine aggregates (NFA) and NCA. In the production of SCC, researchers have investigated the utilization of various industrial byproducts such as FYA, BA, and granulated blast furnace slag as filler materials [20]. Additionally, several studies have explored the potential of C&DW and BA as alternative materials for replacing NCA and NFA in concrete [21, 22]. It is crucial to know the influence of increased FYA replacement on the strength and hydration characteristics of concrete. FYA replaces at least 30% of the cement content, the resulting concrete is stated to as high-volume fly ash (HVFYA) concreteb [9, 23]. FYA exhibits promise as a substitute material that can address the growing requirement of cement and serve as a filler ingredient in SCC [20].

Furthermore, high-volume fly ash self-compacting concrete (HVFYA-SCC) has gained worldwide recognition due to its sustainable nature, cost-effectiveness, and improved durability[8-10]. In this regard, BA has emerged as a promising alternative, as it shares a similar particle size with NFA [24]. Substituting up to 20% of NFA with BA improve the mechanical and durability characteristics of both SCC and conventionally vibrated concrete [9]. However, the inclusion of BA in SCC may lead to a noticeable drop in mechanical and durability characteristics related to conventional SCC [25-27]. A study by Khodair and Bommareddy (2017) [28]examined the mechanical properties of HVFYA-SCC mixes with 50% FYA as supplementary cementitious material and replacement of NCA with RCA (25%-100%). The results exhibited the mechanical characteristics of HVFYA-SCC mixes reduced by approximately 60% with 100% RCA. Similarly, Khodair and Luqman (2017)[29] obtained comparable outcomes for the mechanical strengths of HVFYA-SCC mixes incorporating RCA at levels of 25% to 75% and 70% FYA replacement of cement. The incorporation of RCA influences the strength characteristics, leading to an overall decrease in mechanical properties limited to around 4% [30].

The SCC mix containing 50% BA and 50% FYA exhibited greater mechanical strength after 90 days of curing w.r.t. the control mix. This enhancement accredited to the pozzolanic reaction among BA and cement particles, which contributes to improved strength characteristics [15, 31-35] However, higher concentrations of FYA and BA have shown a decrease in mechanical properties. The higher content of porous BA resulted in increased porosity, leading to a weakening of the microstructure of the material [36]. Few studies have investigated the incorporation of both BA and RCA in HVFYA-SCC. According to Singh et al. (2019) [9], incorporating 10% BA and 30% FYA along with RCA (0-100%) resulted in improvements in compressive, split tensile strength and electrical resistivity for HVFYA-SCC mixes, with noticeable improvements observed for mixes containing up to 50% RCA. In addition, longer curing periods have been found to enhance the electrical resistivity value of HVFYA-SCC mixes, which contain 10% BA and 25% RCA, and 50% FYA. The existence of BA and FYA in SCC mixes leads to additional pozzolanic action and pore-refining action after higher curing ages [10, 37]. According to sorptivity test results, the initial water absorption increased by 66% with 50% RCA and 10% BA w.r.t.

control HVFYA-SCC mix [10]. Therefore, based on the available literature, the current study aimed to investigate the fresh, mechanical and durability characteristics of HVFYA-SCC incorporating RCA and BA.

2 Research significance

Previous research has identified a lack of information on the influence of combining BA and RCA on HVFYA-SCC. Although there have been a few studies on the use of BA and RCA as NFA and NCA substitutions, respectively, in HVFYA-SCC, there is still a lag in identifying the potential of this area. Moreover, the inability to know detailed information about BA and RCA obtained from different sources is generally quoted as an obstacle to their utilization, particularly in restricted and non-restricted applications. The current experimental study attempts to establish the feasibility of developing non-conventional HVFYA-SCC (with BA and RCA) corresponding to hardened characterization. Furthermore, this challenge will assuredly support quality and quantity assurance and increase confidence factual utilization of BA and RCA as primary and secondary alternative materials in HVFYA-SCC. The valuable recycling of RCA and direct use of BA will further assist numerous entities in achieving sustainability goals and will certainly offer environmental advantages linked particularly with dwindling virgin materials and decreased landfill use.

3 Experimental programs

3.1 Mix proportions

HVFYA-SCC was prepared using various materials, including OPC 43-grade, Class-F FYA, NFA, BA, NCA, and RCA. The OPC and FYA met the standards of IS:8112 (2013) [38] and ASTM C 618 (2014) [39], respectively. Figure 1(a) illustrates the particle size gradations of OPC and FYA used in the study. The physical characteristics of the materials are presented in Table 1, while Table 2 provides their chemical properties. The NFA used in the research adhered to the specifications of IS:383 (2016) [40] and belonged to Zone II. BA, obtained from a thermal power plant in Ropar, replaced NFA at varying percentages. NFA and NCA were sourced from the Trehti quarry in Pathankot, India. In a surface-saturated dry condition, NCA was used in proportions of 25%, 42%, and 33% for sizes 6.36 mm, 10 mm, and 12.5 mm, respectively. RCA replaced NCA at 0%, 25%, and 50% and was obtained by crushing and sieving tested concrete specimens following IS 383-2016 guidelines in the Structures Testing Laboratory of the institute. The physical characteristics of these aggregates are listed in Table 3, while Figure 1(b) illustrates the particle size gradation of NFA, NCA, RCA, and BA particles. To achieve the desired HVFYA-SCC, a high-range water-reducing superplasticizer (SP), specifically MasterGlenium 51, was used in varying amounts relative to the weight of the binder under IS:9103 (1999)[41] standards. In the current experimental program, in total ten (10) numbers of HVFYA-SCC combinations were made. It was pre-decided before the actual cast of specimens that each of the designed HVFYA-SCC mix would result in at least compressive strength of 25 N/mm^2 (after 28 days of curing) as the same is generally consider under category of structural grade concrete. Herein, the basic mix proportion for HVFYA-SCC was developed on the basis of Nan-Su Method [42].

Table 1 - Chemical properties of FYA, OPC and BA

Chemical properties	FYA	OPC	BA
SiO_2	60.57	20.89	20.89
Al_2O_3	26.92	5.88	5.88
Fe_2O_3	5.01	3.99	3.99
MgO	0.83	0.93	0.93
CaO	1.43	60.58	60.58
SO_3	0.22	2.83	2.83
K_2O	1.31	1.12	1.12
Na_2O	0.12	0.81	0.81
TiO_2	1.69	0.22	0.22
Loss of Ignition	1.82	2.01	2.01

Table 2 - Physical properties of FYA, OPC and BA

Physical properties	FYA	OPC	BA
Standard consistency (%)	-	32	-
Initial setting time (min)	-	62	-
Final setting time (min)	-	270	-
Soundness (mm)	-	1.0	-
Compressive strength (MPa)			
3 days	-	24.6	-
7 days	-	34.3	-
28 days	-	45.2	-
Specific gravity	2.1	3.15	2.09

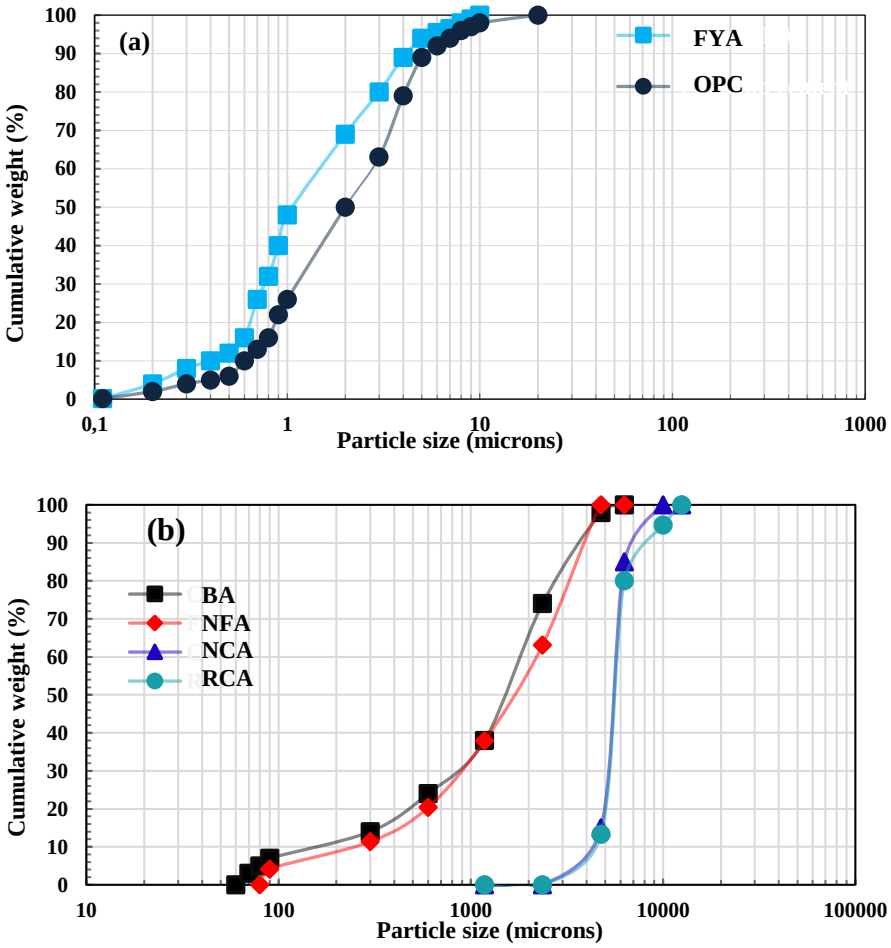

Fig. 1 – Particle size gradation: (a) FYA and OPC, (b) BA, NFA, NCA and RCA

Table 3 – P hysical properties of BA, RCA, NFA and NCA

Properties	NFA	NCA	BA	RCA
Water absorption (%)	1.2	0.68	30	5.65
Fineness modulus	3.98	6.9	1.52	6.8
Specific gravity	2.75	2.64	2.09	2.44

3.2 Materials used

For this study, a total of ten different HVFYA-SCC mixes were prepared. The control mix, CFB0-R0, served as the baseline and consisted of a constant binary blend of 40% OPC and 60% FYA, utilizing 100% NFA and 100% NCA. The remaining mixes incorporated variations with the replacement of NCA ranging from 25% to 50% with RCA and NFA replacement ranging from 10% to 30% with BA. The mix proportions of the HVFYA-SCC mixes are provided in Table 4. All the HVFYA-SCC mixes were prepared following the guidelines of EFNARC 2005 [43]. A fixed water-to-binder ratio of 0.25 and a total binder content of 688 kg/m^3, 887 kg/m^3 of NFA, and 711 kg/m^3 of NCA were maintained. The superplasticizer quantity varied across the HVFYA-SCC mixes, ranging from 0.75% to 1.45% by weight of the binder, as outlined in Table 5. The quantity of SP was varied in each of the mix depending upon the nature (BA/RCA) and content (% replacement level) of ingredients used. For example, in HVFYA-SCC mix CFB10-R0 the SP content was 0.82% (lower) while SP in HVFYA-SCC mix CFB30-R25 was 1.4% (higher) of the binder by weight.

It is important to mention here that higher the replacement of NFA with BA and NCA with RCA has increased the need of SP in the designed mixes in order to satisfy the mandatory guidelines. Similarly, the SP ratio varies from 0.75 to 1.45% for the all the designed HVFYA-SCC mixes investigated in this study however, the mentioned range of SP was calculated and fixed during the trials which was later implied during final cast of HVFYA-SCC mixes.

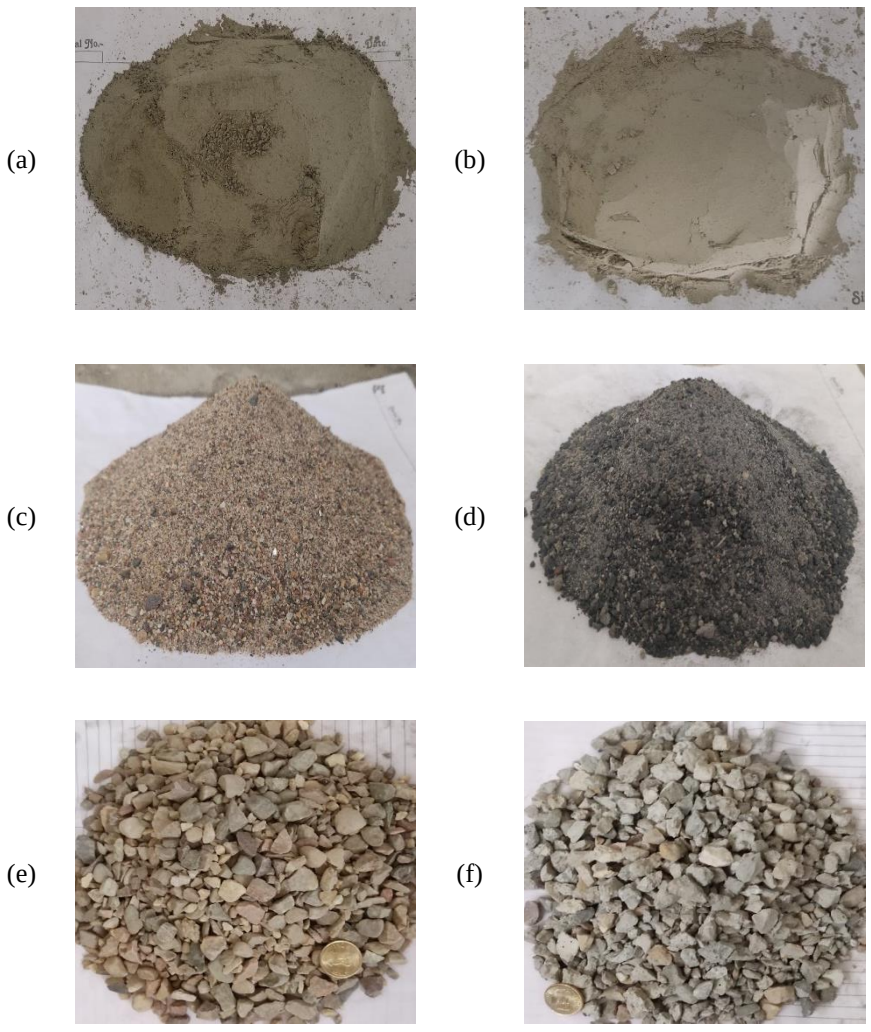

Fig. 2 – Materials used in the investigation: (a) OPC, (b) FYA, (c) NFA, (d) BA, (e) NCA, (f) RCA

Table 4 – Details mix proportions of HVFYA-SCC mixes in kg/m3

S no	Mix ID	OPC	FYA	NFA	BA	NCA	RCA	Water	SP
1	CFB0-R0	275.2	412.8	887	0	711	0	170	5.16
2	CFB10-R0	275.2	412.8	798.3	88.7	711	0	170	5.64
3	CFB10-R25	275.2	412.8	798.3	88.7	533.25	177.75	170	6.54
4	CFB10-R50	275.2	412.8	798.3	88.7	355.50	355.50	170	6.88
5	CFB20-R0	275.2	412.8	709.6	177.4	711	0	170	7.57
6	CFB20-R25	275.2	412.8	709.6	177.4	533.25	177.75	170	8.26
7	CFB20-R50	275.2	412.8	709.6	177.4	355.50	355.50	170	8.60
8	CFB30-R0	275.2	412.8	620.9	266.1	711	0	170	8.94
9	CFB30-R25	275.2	412.8	620.9	266.1	533.25	177.75	170	9.63
10	CFB30-R50	275.2	412.8	620.9	266.1	355.50	355.50	170	9.98

Table 5 – Results of fresh properties

S no	Mix ID	Slump flow		V-funnel	J-ring		L-box	SP
		Flow spread (*mm*)	T_{500} (*sec*)	(*sec*)	Flow spread (*mm*)	T_{500} (*sec*)	H_2/H_1	(*%*)
1	CFB0-R0	740	3.6	8	735	3.9	0.97	0.75
2	CFB10-R0	722	3.9	10.3	715	4.2	0.96	0.82
3	CFB10-R25	716	4.1	11.2	710	4.4	0.94	0.95
4	CFB10-R50	710	4.4	11.9	705	4.8	0.92	1.00
5	CFB20-R0	715	4.1	11.4	710	4.5	0.95	1.10
6	CFB20-R25	710	4.5	12.1	705	4.7	0.93	1.20
7	CFB20-R50	705	4.7	12.8	700	5.0	0.91	1.25
8	CFB30-R0	711	4.6	12.5	705	4.8	0.94	1.30
9	CFB30-R25	705	4.9	13.3	695	5.2	0.91	1.40
10	CFB30-R50	700	5.2	14	690	5.8	0.90	1.45

3.3 Test methods

The assessment of fresh characteristics for HVFYA-SCC mixes followed the EFNARC (2005) [43] guidelines, which involved tests such as slump flow to determine filling ability, V funnel and T500 for viscosity, and J ring and L box to evaluate passing capability. Compressive strength testing was determined using cubic samples measure 100 mm x 100 mm x 100 mm by IS 516 (2021) [44], while split tensile strength was carried out on cylindrical samples with dimensions of 100 mm x 200 mm following IS 5816 (1999) [45]. The mechanical properties were tested at 7, 28, 56, 90, and 120 days of curing. Non-destructive testing methods were employed to assess the homogeneity, robustness, cracks, voids, and pores of HVFYA-SCC. The ultrasonic pulse velocity (UPV) test was conducted on cubic samples measuring 100 mm x 100 mm x 100 mm as per IS:13311 (Part 1) 1992 [46]. Sorptivity testing, which examines water penetration through capillary pores, was performed on disc-shaped samples dia. of 100 mm and a width of 50 mm, obtained from cylindrical samples using a diamond saw cutter. The specimens were conditioned according to ASTM C 1585 (2004) [47]. The electrical resistivity of HVFYA-SCC mixes was measured using a Resipod resistivity meter, following AASHTO T 358 (2022) [48]. Cylindrical samples of 100 mm x 200 mm were used for electrical resistivity testing. Durability characteristics were evaluated after 28, 56, 90, and 120 days of curing.

4 Results and discussions

4.1 Fresh properties

The fresh properties of the HVFYA-SCC mixes were assessed using the EFNARC [43] guidelines. The V funnel, Slump flow, J ring, and L box test results are presented in Table 5, demonstrating the fresh qualities of the CBA-based HVFYA-SCC mixes. The results of the HVFYA-SCC mixes reveal that, in comparison to the control mix, adding BA and RCA decreases flowing ability. The incorporation of 30% BA revealed a negative effect on the slump values, while the maximum reduction (nearly 5%) was noted in the mix CFB30-R50 compared to CFB0-R0. The concrete's capacity to pass was evaluated using the L-box test. All HVFYA-SCC mixes had blocking ratio values between 0.90 and 0.97, which complied with EFNARC 2005 requirements [43]. Similar findings as noticed above; J-Ring tests were noted for mix CFB30-R50 wherein the reduction was limited to around 6% compared to control HVFYA-SCC mix (CFB0-R0).

Further, T500 and V-funnel were used to estimate the viscosity of the SCC mixes. The V-funnel results demonstrate that the SCC mixes satisfy the flow criteria, as advised in the EFNARC 2005 standards [43]. On the contrary, adding BA and RCA has significantly shortened the flow time. The flow time for mix CFB30-R50 has been increased by 75% (V-funnel) compared to the control HVFYA-SCC mix (CFB0-R0). The inclusion of irregular and porous BA particles offers higher inter particle friction resulting in decrease of workability characteristics of concrete [49-51]. Likewise, the adhered residual mortar on the surface of RCA is generally treated as rough and highly of porous nature leading to excessive inter particle friction and higher water demand [52, 53]. Therefore, the effect of inter particle friction becomes more dominant wherein BA and RCA are used as combined replacement of NFA and NCA in concrete.

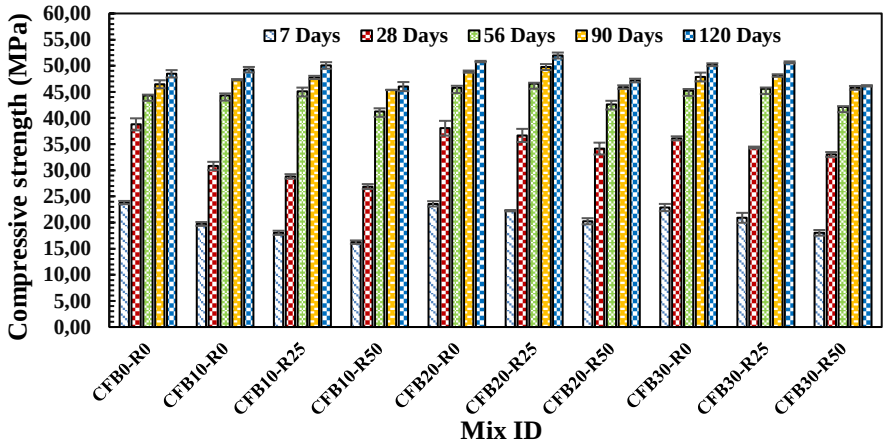

Fig. 3 – Compressive strength of HVFYA-SCC mixes

4.2 Compressive strength

Figure 3 displays the compressive strength (CS) results for all the HVFYA-SCC mixes at different curing periods. The data showed a general decline in CS as the BA concentration increased after 7 days of curing. Figure 3 revealed a decrement of 17%, 1%, and 4% for HVFYA-SCC mixes CFB10-R0, CFB20-R0, and CFB30-R0, correspondingly, reference to the HVFYA-SCC mix CFB0-R0. This pattern was too observed for CS at 28 days. The decrease in HVFYA-SCC mixes during the early stages of curing was due to the decline in the heat of hydration of cement and the pozzolanic activity of FYA and BA with cement. [27, 36]. However, after 56 days, the CS of the HVFYA-SCC mixes was observed to be equal to the HVFYA-SCC CFB0-R0 mix. The CS of HVFYA-SCC mixes with varying amounts of BA and curing time was analysed in Figure 3. The results showed that CFB10-R0, CFB20-R0, and CFB30-R0 mixes slightly increased by up to 3% in CS than the HVFYA-SCC CFB0-R0 mix after 56 days. The similar trend was detected for 10% to 30% BA, where CS increased to 7% with a curing time of 90 and 120 days. On the other hand, when 25% and 50% RCA were added to the 10% BA mixes, a decrease in CS was observed with reference to HVFYA-SCC mix CFB0-R0. Specifically, the CS at 7 days dropped from 19.73 MPa for the CFB10-R0 mix to 18.03 MPa and 16.24 MPa, respectively, when 25% and 50% of the RCA were used as NCA. HVFYA-SCC mixes CFB20-R0 and CFB30-R0 showed a decrement in CS with 25% and 50% RCA up to 28 days

curing period. The reduced CS can be accredited to old, residual adhering mortar in RCA, which contributes to the poor structural characteristics of materials at higher RCA content levels [54, 55].

Furthermore, after 56 days of curing age, the CS of the HVFYA-SCC mix CFB10-R0 improved slightly from 44.32 MPa to 45.13 MPa with 25% replacement of RCA. BA and FYA may increase CS in the HVFYA-SCC mix with lower RCA concentrations due to additional pozzolanic reactivity [9]. However, 50% RCA had the contrary effect; the CS of CFB10-R50 decreased up to 7% after 56 days of curing. The weak adhered mortar in RCA reduces overall CS, which could be attributed to the maximum RCA content and poor structural properties [54, 55]. HVFYA-SCC mixes with 20% and 30% BA showed similar trends, where extended curing time resulted in higher CS when 25% RCA replaced as NCA, while 50% RCA replacement resulted in reduced CS. The CS of the CFB20-R25 mix enhanced from 22.27 MPa at 7 days of curing to 51.96 MPa at 120 days. As per the results, the CFB20-R25 mix had higher strength than the HVFYA-SCC mix CFB0-R0 at 120 days of curing (48.46 MPa). Similarly, mix CFB30-R25 exhibited 4% higher CS after 120 days of curing with reference to HVFYA-SCC mix CFB0-R0, as depicted in Figure 3. Overall, the study revealed that the CS of a 20% BA-based mix (CFB20-R25) was significantly increased with 25% RCA. This was in contrast to mixes with 10% and 30% replacement levels of BA with NFA. This rise in CS at the later curing period was attributed to the pozzolanic effect of BA and FYA with cement particles [50, 56]. In contrast, the addition of 50% RCA as an NCA leads to a significant reduction in CS for all BA mixes, including CFB10-R50, CFB20-R50, and CFB30-R50, at different curing ages, which is much lesser than the HVFYA-SCC mix (CFB0-R0). After 120 days of curing, the CSs of HVFYA-SCC mix that contained 50% RCA, such as CFB10-R50, CFB20-R50, and CFB30-R50, were measured at 46.01 MPa, 47.17 MPa and 46.16 MPa correspondingly, w.r.t. the HVFYA-SCC mix CFB0-R0 (48.46 MPa). As mentioned earlier the weaker, porous, feeble and cracked RCA resulted in lower CS particularly for higher replacement HVFYA-SCC mixes [54, 55].

4.3 Split tensile strength

According to Figure 4, the results of the split tensile strength (TS) tests indicated a decrease of 9%, 1%, and 2% for the CFB10-R0, CFB20-R0, and CFB30-R0 mixes, respectively, compared to the reference HVFYA-SCC mix CFB0-R0 after 7 days of curing. This decrease in TS during the early stages of curing can be attributed to a reduction in cement hydration and the pozzolanic activity of FYA and BA with cement particles [27, 36]. There are two probable reasons for such behaviour: Firstly; the replacement of stronger material (NFA) with weaker material (BA) and secondly; non-initiation of pozzolanic action of BA after initial ages of curing. Such trends are also available in the literature which are duly co-related with the current experimental results. On the other side, the higher replacement levels i.e., 20% and 30% BA impart filler action or pore refinement in HVFYA-SCC mixes making the denser forms, thereby resulting in improved strength values.

Similar trends were observed for the TS at 28 days. However, at 56 days, the CFB10-R0, CFB20-R0, and CFB30-R0 mixes exhibited marginally increases of 1% compared to the HVFYA-SCC mix (3.59 MPa). This trend was also observed in mixes containing 10% BA, where the split tensile strength continued to increase from 56 days to 120 days of curing, as shown in Figure 4. This could be attributed to the synergistic effect of FYA and BA, which contribute to the pozzolanic reaction with cement particles in the HVFYA-SCC mix after higher ages [50, 56].

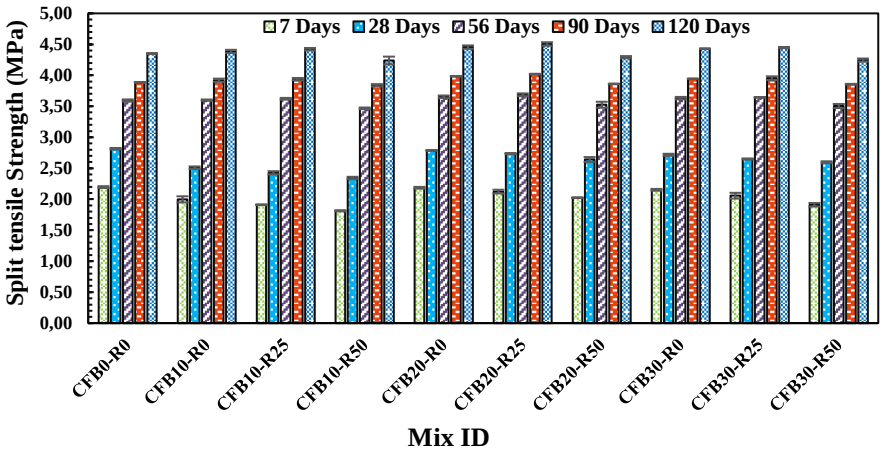

Fig. 4 – Split tensile strength of HVFYA-SCC mixes

The TS of the 10% BA mix with 25% and 50% RCA was lower than that of the HVFYA-SCC mix CFB0-R0 after 7 days of curing. Specifically, the TS for the CFB10-R25 and CFB10-R50 mixes decreased by 13% and 17% respectively, compared to the HVFYA-SCC mix CFB0-R0 (2.20 MPa). After 28 days, the TS of the CFB10-R25 and CFB10-R50 mixes decreased by 13% and 16% respectively, compared to the HVFYA-SCC mix CFB0-R0 (2.81 MPa). However, with increasing curing age, the CFB10-R25 mix exhibited a marginal increase of 0.8% in TS compared to the HVFYA-SCC mix CFB0-R0 at 56 days (3.59 MPa). This can be attributed to additional pozzolanic reactions facilitated by the presence of BA and FYA with cement particles, resulting in improved TS in HVFYA-SCC mixes with lower RCA content [9]. On the other hand, the CFB10-R50 mix showed a lower TS of 3.47 MPa w.r.t. the HVFYA-SCC mix CFB0-R0, and this trend persisted as the 56 days. The observed decline in TS in mixes with 50% RCA can be accredited to the presence of old, residual adhering mortar in the RCA, which adversely affects the material's structural properties as the RCA content rises [54, 55]. Similarly, the HVFYA-SCC mixes with 20% and 30% BA, along with 25% RCA, exhibited higher TS compared to the HVFYA-SCC mixes with 50% RCA as the curing period extended up to 56 days.

Figure 4 demonstrates that at 90 days of curing, the CFB20-R25 and CFB30-R25 mixes exhibited TS that were 3% and 2% higher, correspondingly, than the HVFYA-SCC mix CFB0-R0. This trend continued at 120 days of curing. The significant improvement in TS at later curing ages, particularly in mixes with 10-30% BA replacement for NFA, can be attributed to the additional pozzolanic reaction between BA, FYA, and cement particles [9, 50, 56]. However, the presence of weak bonding between the mortar and porous aggregate in all HVFYA-SCC mixes with 50% RCA, such as CFB10-R50, CFB20-R50, and CFB30-R50, may lead to a slight decrease in TS w.r.t. HVFYA-SCC mixes with 25% RCA [50, 55].

4.4 Ultrasonic pulse velocity

Ultrasonic pulse velocity is a non-destructive testing method that provides valuable insights into the quality of concrete. It is capable of detecting defects such as cracks and voids, assessing the uniformity of concrete, and monitoring changes in the concrete structure and quality over time. In the study conducted on HVFYA-SCC mixes, Figure 5 displays the UPV values at curing intervals of 7, 28, 56, 90, and 120 days. After 7 days of curing periods, the UPV values of all HVFYA-SCC mixes were lesser than the HVFYA-SCC mix CFB0-R0. The UPV values of the HVFYA-SCC mixes CFB10-R0, CFB20-R0, and CFB30-R0 were lesser by 3%, 0.17%, and 0.6%, respectively, than the HVFYA-SCC mix CFB0-R0. As depicted in Figure 5, the HVFYA-SCC mixes displayed UPV values ranging from 3356 m/s to 3561 m/s after 7 days of curing. Interestingly, the UPV values of the HVFYA-SCC mixes incorporating BA showed slight improvements over time, particularly with an increase in BA content. This indicates that the concrete exhibits good quality in terms of homogeneity, uniformity, and density. At 120 days, the UPV values for CFB10-R0, CFB20-R0, and CFB30-R0 were marginally increased by 0.3%, 0.8%, and 0.6%, respectively, then the HVFYA-SCC mix (CFB0-R0), owing to a significant reduction in permeable pore space in BA-based HVFYA-SCC mixes [50].

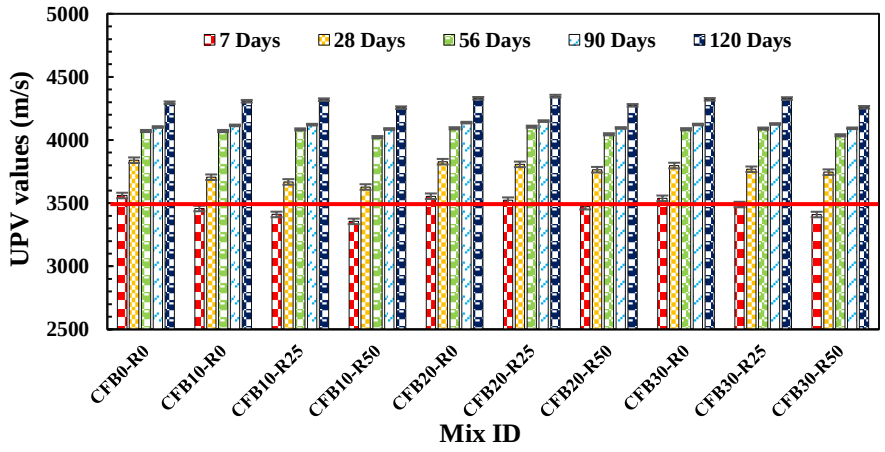

Fig. 5 – UPV test results of HVFYA-SCC mixes

However, when 25% and 50% RCA were included with 10% BA, the UPV values decreased marginally by 4% and 6% for CFB10-R25 and CFB10-R50, respectively, compared to CFB0-R0 mix, after a 7-days curing period. After 120 days, the UPV values for CFB10-R25 demonstrated 1% higher UPV values than CFB0-R0, while CFB10-R50 was marginally lower

(0.9%) compared to CFB0-R0 mix. Including 25% RCA resulted in higher UPV values due to decreased permeable behavior in BA-based HVFYA-SCC mixes [9, 50]. Similarly, the UPV values for mixes containing 20% and 30% BA showed an improvement with 25% RCA and a negligible decrease with 50% RCA as the curing period increased. Based on the findings, it can be inferred that 25% RCA replacement significantly enhanced the performance with 20% BA, with higher UPV values compared to those prepared with 10% and 30% BA. After 28 days of curing, the UPV values of the HVFYA-SCC mixes ranged from 3628 m/s to 3840 m/s. As the curing period progressed, the UPV values further increased. At 56 days, the UPV values ranged from 4023 m/s to 4106 m/s, at 90 days they ranged from 4088 m/s to 4150 m/s, and at 120 days they ranged from 4257 m/s to 4349 m/s. As per IS:13311 (Part 1) 1992 [46], all HVFYA-SCC mixes exhibited 'good' quality concrete at 7, 28, 56, 90 and 120 days of curing. Using BA and RCA instead of NFA and NCA, respectively, can produce concrete in the 'good' category as recommended by IS:13311 (Part 1) 1992 [46] and supported by literature and current results [8-10, 50]

4.5 Sorptivity

The rate of water absorption was measured using sorptivity, which involves determining the increase in mass of a sample over time when only a single surface is exposed to water. Lower water absorption is a sign of higher concrete durability. Figure 6 presents the sorptivity results for different HVFYA-SCC mixes. After 28 days of curing, the control HVFYA-SCC mix showed a minimum sorptivity value of 0.0140 mm/s$^{1/2}$. The utilization of 10%, 20%, and 30% BA as the partial amount of NFA in the HVFYA-SCC mix showed maximum sorptivity value ranging from 0.0141 to 0.0148 mm/s$^{1/2}$ for 28 days. After 56 days, the sorptivity value for HVFYA-SCC mixes CFB10-R0, CFB20-R0, and CFB30-R0 decreased by 0.2%, 2% and 1%, respectively, than the HVFYA-SCC mix (CFB0-R0) due to the filling ability in addition pozzolanic reaction of BA and FYA with cement particles [9].

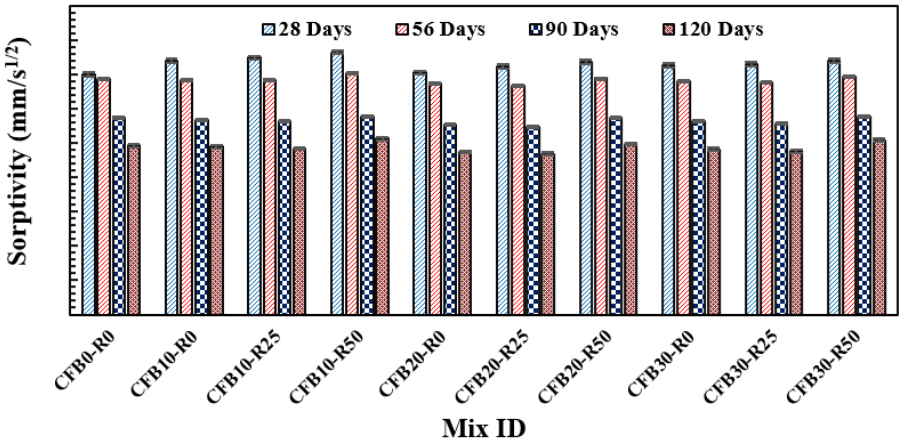

Fig. 6 – Sorptivity test results of HVFYA-SCC mixes

The sorptivity value increased with the inclusion of 25% RCA and 50% RCA with 10%, 20%, and 30% BA as partial replacement of NFA than HVFYA-SCC mix CFB0-R0 after 28 days periods of curing. At 56 days, the 25% RCA as NCA significantly increased resistance against capillary absorption for all HVFYA-SCC mixes. Among all HVFYA-SCC mixes, CFB20-R25 was more resistant to capillary absorption, about 3% of the reduction in sorptivity was noticed than HVFYA-SCC mix CFB0-R0 after 56 days curing stage. A similar decline in sorptivity was noticed for 90 and 120 days. The drop in sorptivity of HVFYA-SCC mixes CFB10-R25 and CFB30-R25 varied from 0.0149 mm/s$^{1/2}$ to 0.0096 mm/s$^{1/2}$ and 0.0146 mm/s$^{1/2}$ to 0.0095 mm/s$^{1/2}$, respectively, corresponding to the 28 to 120 days curing age. Incorporating BA and RCA in place of NFA and NCA in HVFYA-SCC mixes may have resulted in additional pozzolanic reactions between BA, FYA, and cement, leading to the lower capillarity coefficients observed [10, 57]. The sorptivity value of HVFYA-SCC mixes with 50% RCA increased by 3%, 0.5%, and 1.5% for HVFYA-SCC mixes CFB10-R50, CFB20-R50 and CFB30-R50, respectively, at 56 days periods of curing. A similar trend of sorptivity of HVFYA-SCC mixes with 50% RCA was noticed for 90 and 120 days. The observed trend of increasing sorptivity values could be attributed to weak cementitious paste or adhered mortar on the surface of RCA. This weak paste may increase porosity and permeability, leading to higher sorptivity values [9, 57].

4.6 Electrical resistivity

Electrical resistivity indicates the ionic transfer within the concrete microstructure, influencing its durability. Figure 7 presents the electrical resistivity for various HVFYA-SCC mixes. After 28 days, the HVFYA-SCC mix (CFB0-R0) showed the maximum electrical resistivity value of 19.34 KΩcm. The utilization of 10%, 20%, and 30% BA as partial replacement of NFA in the HVFYA-SCC mix showed minimum electrical resistivity value ranging from 17.33 to 19.13 KΩcm for 28 days. After 56 days, the electrical resistivity for HVFYA-SCC mixes CFB10-R0, CFB20-R0 and CFB30-R0 improved marginally by 1%, 8% and 3% to the HVFYA-SCC mix CFB0-R0 owing to the filling ability and additional pozzolanic reaction of BA and FYA with cement particles [9]. The electrical resistance value was reduced by including 25% RCA and 50% RCA with 10%, 20%, and 30% BA as partial replacement of NFA than the HVFYA-SCC mix CFB0-R0 after 28 days. The electrical resistivity was decreased as the quantity of RCA was increased up to 50%. For HVFYA-SCC mixes CFB10-R25 and CFB10-R50, a decrement of 12% and 14% was experienced, correspondingly, at curing of 28 days w.r.t. HVFYA-SCC mix CFB0-R0. Likewise, it can be seen that 20% and 30% BA mixes with 25% RCA and 50% RCA at 28 days of the curing stage.

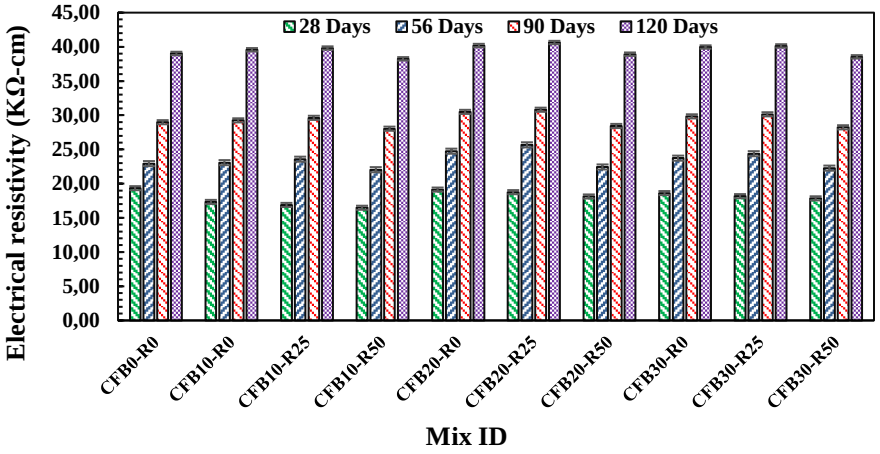

Fig. 7 – Electrical resistivity test results of HVFYA-SCC mixes

After 56 days curing period, the 25% RCA as replacement of NCA significantly increased electrical resistivity values with 10%, 20%, and 30% BA as partial replacement of NFA in HVFYA-SCC mixes. Among all, HVFYA-SCC mixes CFB20-R25 have 12% more electrical resistivity values with reference to HVFYA-SCC mix CFB0-R0 for 56 days of curing. A similar trend of electrical resistivity of HVFYA-SCC mixes with 25% RCA was observed after 90 and 120 days. The increase in electrical resistivity of HVFYA-SCC mixes CFB10-R25 and CFB30-R25 varied from 16.89 KΩcm to 39.82 KΩcm and 18.17 to 40.14 KΩcm, respectively, corresponding to the 28 to 120 days curing age. The additional pozzolanic reactions between BA, FYA, and cement may cause the increment of electrical resistivity values of HVFYA-SCC mixes when BA as NFA and RCA as NCA are replaced, respectively [10, 57]. The electrical resistivity value of HVFYA-SCC mixes with 50% RCA decreased by 4%, 2%, and 3% for HVFYA-SCC mixes CFB10-R50, CFB10-R50, and CFB30-R50, correspondingly, at 56 days. The trend may be accredited to the weak cementitious paste or adhered mortar on the surface of RCA, potentially leading to decreased electrical resistivity values [9, 54, 57]. A similar trend of electrical resistivity of HVFYA-SCC mixes with 50% RCA was observed after 90 and 120 days. The HVFYA-SCC mixes exhibited electrical resistivity values varying from 16.48 KΩcm to 19.34 KΩcm after 28 days of curing and from 22.04 KΩcm to 25.67 KΩcm, 28.03 KΩcm to 30.81 KΩcm and 38.25 KΩcm to 40.63 KΩcm at 56, 90 and 120 days respectively. According to AASHTO T 358 (2022)[57], all HVFYA-SCC mixes demonstrated low and negligible risk of corrosion after 28, 56, 90 and 120 days of the curing stage.

4.7 Mathematical relationships

The linear regression analysis has established a correlation between mechanical characteristics and durability characteristics [58]. Previous studies have reported R^2 values of 0.7, indicating a strong correlation among these characteristics [59, 60].

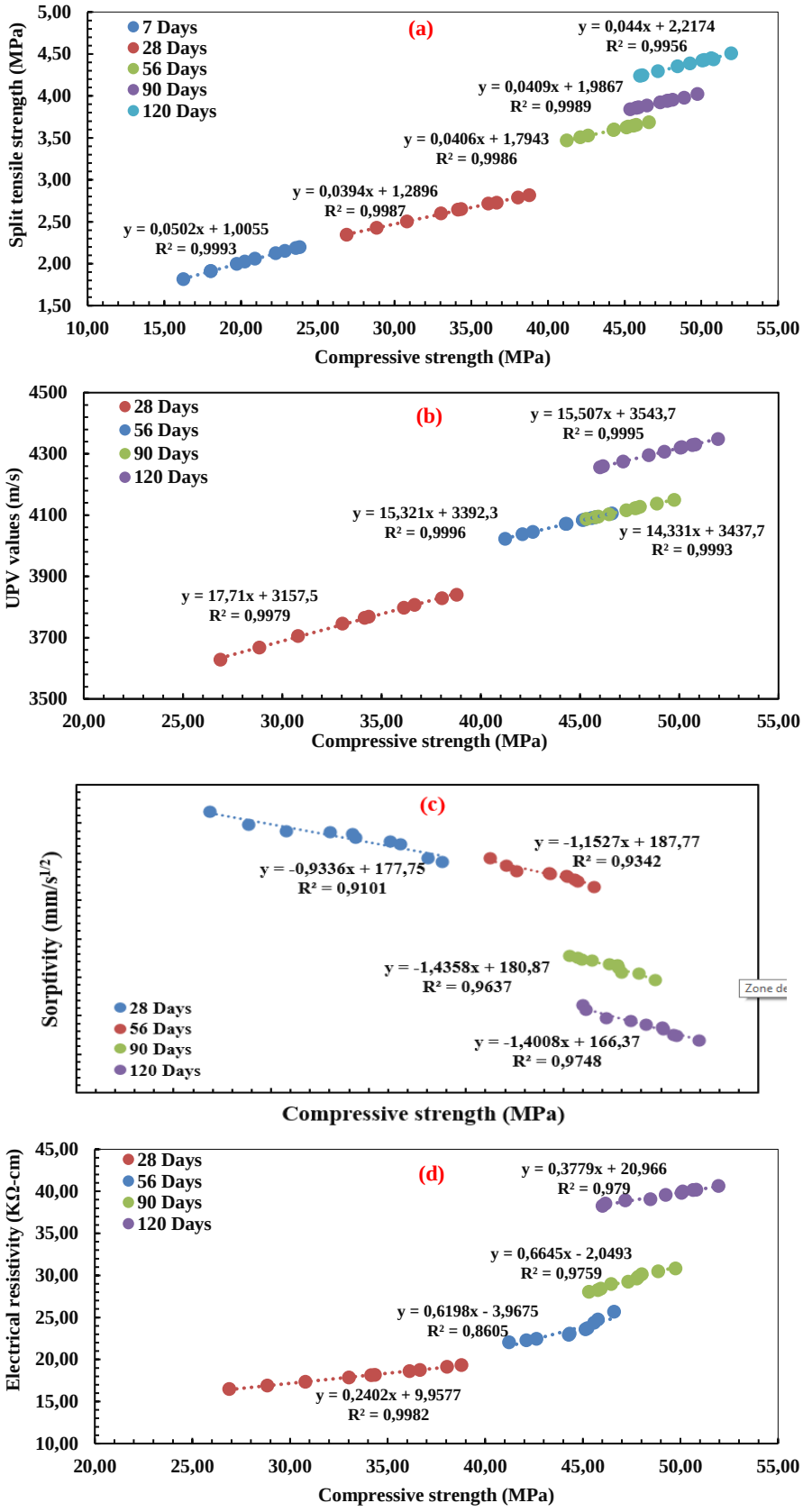

Fig. 8 – Relationship between compressive strength versus (a) split tensile strength, (b) UPV values, (c) sorptivity, (d) electrical resistivity

Additionally, earlier research has suggested that split tensile strength exhibits a linear relationship with compressive strength in HVFYA-SCC mixes [30, 36, 50, 61]. Figure 8(a) displays the outcomes of the present study, demonstrating a

strong correlation amongst compressive strength and split tensile strength, with R^2 values amongst 0.9956-0.9993. Significant correlations were observed in Figures 8(b), 8(c), and 8(d) between compressive strength versus UPV values, compressive strength versus sorptivity and compressive strength versus electrical resistivity were obtained with R^2 values ranging from 0.9970-0.9996, 0.9101-0.9748 and 0.8605-0.9982, respectively [30, 36, 50, 59, 62]. Table 6 presents R^2 values and equation of linear regression relationship co-efficient between mechanical properties and durability properties.

Table 6 – Correlation coefficients of mechanical and durability properties

Properties	Curing days	R^2	Linear regression equations
Compressive strength v/s split tensile strength	7	0.9993	y = 0.0502x + 1.0055
	28	0.9987	y = 0.0394x + 1.2896
	56	0.9986	y = 0.0406x + 1.7943
	90	0.9989	y = 0.0409x + 1.9867
	120	0.9956	y = 0.044x + 2.2174
Compressive strength v/s UPV values	28	0.9970	y = 17.71x + 3157.5
	56	0.9996	y = 15.321x + 3392.3
	90	0.9993	y = 14.331x + 3437.7
	120	0.9995	y = 15.507x + 3543.7
Compressive strength v/s sorptivity	28	0.9101	y = -0.9336x + 177.75
	56	0.9342	y = -1.1527x + 187.77
	90	0.9637	y = -1.4358x + 180.87
	120	0.9748	y = -1.4008x + 166.37
Compressive strength v/s electrical resistivity	28	0.9982	y = 0.2402x + 9.9577
	56	0.8605	y = 0.6198x - 3.9675
	90	0.9759	y = 0.6645x - 2.0493
	120	0.9790	y = 0.3779x + 20.966

5 Conclusions

This investigation aimed to evaluate the fresh properties, mechanical properties and durability properties of the HVFYA-SCC mixes containing RCA as NCA and BA as NFA. The ensuing conclusions are based on the results of the study:

- Adding BA to the HVFYA-SCC mix with increased RCA content required a higher dosage of SP than the HVFYA-SCC mix CFB0-R0.

- HVFYA-SCC mix with 10% BA and 50% RCA showed 30% lower compressive strength compared to the HVFYA-SCC mix (CFB0-R0) at 7 and 28 days of curing. However, after 56, 90 and 120 days of curing, mix CFB20-R25 revealed the 5%, 7% and 7% respectively, higher compressive strength compared to the HVFYA-SCC mix (CFB0-R0).

- Likewise, the split tensile strength of the mix CFB20-R25 was recorded to be 2%, 3% and 3% higher, corresponding to the HVFYA-SCC mix CFB0-R0 at 56, 90 and 120 days, respectively. All HVFYA-SCC mixes exhibited UPV values exceeding 3500 m/s, indicating that the quality of the concrete was ‘good’ at all curing stages.

- After 28 days of curing, the sorptivity of HVFYA-SCC mixes containing 10% BA and 50% RCA was observed 9% more than the HVFYA-SCC mix (CFB0-R0). However, after 56, 90 and 120 days of curing, the CFB20-R25 mix exhibited the most significant 2%, 4% and 5% reduction, respectively in sorptivity.

- The HVFYA-SCC mix CFB10-R50 had 15% lower electrical resistance than the HVFYA-SCC mix CFB0-R0 at 28 days of curing, but mix CFB20-R25 had significantly 12%, 6% and 4% higher electrical resistance than the HVFYA-SCC mix CFB0-R0 at 56, 90 and 120 days of curing age, respectively.

Acknowledgements

The first author of this study would like to acknowledge the Ministry of Education, Government of India, for their financial assistance through a stipend fellowship throughout their Ph.D.

REFERENCES

[1]- W. Tang, M. Khavarian, A. Yousefi, B. Landenberger, H. Cui, Influence of Mechanical Screened Recycled Coarse Aggregates on Properties of Self-Compacting Concrete. Materials (Basel), 16 (2023). doi:doi.org/10.3390/ma16041483.

[2]- B. Wang, L. Yan, Q. Fu, B. Kasal, A Comprehensive Review on Recycled Aggregate and Recycled Aggregate Concrete, Resour. Conserv. Recycl, 171 (2021) 105565. doi:doi.org/10.1016/j.resconrec.2021.105565.

[3]- S. Jain, S. Singhal, N.K. Jain, Construction and demolition waste (C&DW) in India: generation rate and implications of C&DW recycling. International Journal of Construction Management, 21 (2018) 261-270. doi:doi.org/10.1080/15623599.2018.1523300.

[4]- United-Nation, World Urbanization Prospects, Department of Economic and Social Affairs United Nation. (2018).

[5]- R. Sharma, K. Senthil, An investigation on mechanical and microstructural properties of hybrid fiber reinforced concrete with manufactured sand and recycled coarse aggregate. J. Build. Eng., 69 (2023) 106236. doi:doi.org/10.1016/j.jobe.2023.106236.

[6]- A. Coelho, J. de Brito, Environmental analysis of a construction and demolition waste recycling plant in Portugal - Part I: Energy consumption and CO_2 emissions. Waste Manag., 33 (2013) 1258-1267. doi:doi.org/10.1016/j.wasman.2013.01.025.

[7]- M. De Schepper, P. Van den Heede, I. Van Driessche, N. De Belie, Life Cycle Assessment of Completely Recyclable Concrete. Materials (Basel), 7 (2014) 6010-6027. doi:doi.org/10.3390/ma7086010.

[8]- N. Singh, S.P. Singh, Carbonation resistance and microstructural analysis of Low and High Volume Fly Ash Self Compacting Concrete containing Recycled Concrete Aggregates. Constr. Build. Mater, 127 (2016) 828-842. doi:doi.org/10.1016/j.conbuildmat.2016.10.067.

[9]- N. Singh, M. Mithulraj, S. Arya, Utilization of coal bottom ash in recycled concrete aggregates based self compacting concrete blended with metakaolin. Resour. Conserv. Recycl, 144 (2019) 240-251. doi:doi.org/10.1016/j.resconrec.2019.01.044.

[10]- P. Kumar, N. Singh, Influence of recycled concrete aggregates and Coal Bottom Ash on various properties of high volume fly ash-self compacting concrete. J. Build. Eng., 32 (2020) 1-12. doi:doi.org/10.1016/j.jobe.2020.101491.

[11]- R. Kurad, J.D. Silvestre, J. de Brito, H. Ahmed, Effect of incorporation of high volume of recycled concrete aggregates and fly ash on the strength and global warming potential of concrete. J. Clean. Prod. , 166 (2017) 485-502. doi:doi.org/10.1016/j.jclepro.2017.07.236.

[12]- Central Electricity Authority, Central Electricity Authority, Report on Fly Ash Generation at Coal / Lignite Based Thermal Power Stations and its Utilization in the Country for the Year 2020-21. (2021).

[13]- N. Singh, R.U.D. Nassar, K. Shehnazdeep, B. Anjani, Microstructural characteristics and carbonation resistance of coal bottom ash based concrete mixtures. Mag. Concr. Res., 74 (2021) 364-378. doi:doi.org/10.1680/jmacr.20.00125.

[14]- I. G. of, Ministry of External Affairs, National Statement by Prime Minister Shri Narendra Modi at COP26 Summit in Glasgow. (2021).

[15]- M.A. Keerio, A. Saand, A. Kumar, N. Bheel, K. Ali, Effect of local metakaolin developed from natural material soorh and coal bottom ash on fresh, hardened properties and embodied carbon of self-compacting concrete. Environ. Sci. Pollut. Res., (2021) 1–31. doi:doi.org/10.1007/s11356-021-14960-w.

[16]- A.M. Rashad, A comprehensive overview about the influence of different admixtures and additives on the properties of alkali-activated fly ash. Mater. Des., 53 (2014) 1005–1025. doi:doi.org/10.1016/j.matdes.2013.07.074.

[17]- N. Ganesan, R. Abraham, S.D. Raj, Durability characteristics of steel fibre reinforced geopolymer concrete. Constr. Build. Mater., 93 (2015) 471-476. doi:doi.org/10.1016/j.conbuildmat.2015.06.014.

[18]- Y. Wu, B. Lu, T. Bai, H. Wang, F. Du, Y. Zhang, L. Cai, C. Jiang, W. Wang, Geopolymer , green alkali activated cementitious material : Synthesis , applications and challenges. Constr. Build. Mater., 224 (2019) 930–949. doi:doi.org/10.1016/j.conbuildmat.2019.07.112.

[19]- N. Singh, S.P. Singh, Reviewing the Carbonation Resistance of Concrete. J. Mater. Eng. Struct., 3 (2016) 35–57.

[20]- M. Uysal, The influence of coarse aggregate type on mechanical properties of fly ash additive self-compacting concrete,. Constr. Build. Mater., 37 (2012) 533–540. doi:doi.org/10.1016/j.conbuildmat.2012.07.085.

[21]- ACI-Committee-211, Guide for Selecting Proportions for High-Strength Concrete with Portland Cement and Fly Ash. ACI Mater. J., 90 (1998) 1-13.

[22]- M. Arezoumandi, J.S. Volz, C.A. Ortega, J.J. Myers, Shear Behavior of High-Volume Fly Ash Concrete versus Conventional Concrete: Experimental Study. J. Struct. Eng., 141 (2015) 1-11. doi:doi.org/10.1061/(asce)st.1943-541x.0001003.

[23]- V.M. Malhotra, P.K. Mehta. High-Performance, High-Volume Fly Ash Concrete. in 3rd Ed. Suppl. Cem. Mater. Sustain. Dev. Inc. Ottawa, Canada,. (2008), 142.

[24]- N. Singh, Shehnazdeep, A. Bhardwaj, Reviewing the role of coal bottom ash as an alternative of cement. Constr. Build. Mater., 233 (2020) 117276. doi:doi.org/10.1016/j.conbuildmat.2019.117276.

[25]- R. Siddique, Compressive strength, water absorption, sorptivity, abrasion resistance and permeability of self-compacting concrete containing coal bottom ash. Constr. Build. Mater., 47 (2013) 1444-1450. doi:doi.org/10.1016/j.conbuildmat.2013.06.081.

[26]- R. Siddique, Kunal, Design and development of self-compacting concrete made with coal bottom ash. J. Sustain. Cem. Mater., 4 (2015) 225-237. doi:doi.org/10.1080/21650373.2015.1004138.

[27]- N.E. Zainal Abidin, M.H. Wan Ibrahim, N. Jamaluddin, K. Kamaruddin, A.F. Hamzah, The effect of bottom ash on fresh characteristic, compressive strength and water absorption of self-compacting concrete. Appl. Mech. Mater., 660 (2014) 145-151. doi:doi.org/10.4028/www.scientific.net/AMM.660.145.

[28]- Y. Khodair, B. Bommareddy, Self-consolidating concrete using recycled concrete aggregate and high volume of fly ash, and slag, . Constr. Build. Mater., 153 (2017) 307-316. doi:doi.org/10.1016/j.conbuildmat.2017.07.063.

[29]- Y. Khodair, Self-compacting concrete using recycled asphalt pavement and recycled concrete aggregate. 12 (2017) 282–287.

[30]- R.B. Singh, S. Debbarma, N. Kumar, S. Singh, Hardened state behaviour of self-compacting concrete pavement mixes containing alternative aggregates and secondary binders. Constr. Build. Mater., 266 (2021) 1-18. doi:doi.org/10.1016/j.conbuildmat.2020.120624.

[31]- A.M. Hasim, K.A. Shahid, N.F. Ariffin, N.N. Nasrudin, M.N.S. Zaimi, Study on mechanical properties of concrete inclusion of high-volume coal bottom ash with the addition of fly ash. Mater. Today Proc. c, (2021) 1–7. doi:doi.org/10.1016/j.matpr.2021.11.400.

[32]- H.A. Alaka, L.O. Oyedele, O.L. Toriola-Coker, Effect of excess dosages of superplasticizer on the properties of highly sustainable high-volume fly ash concrete. Int. J. Sustain. Build. Technol. Urban Dev., (2016) 1–14. doi:doi.org/10.1080/2093761X.2016.1167643.

[33]- C.H. Huang, S.K. Lin, C.S. Chang, H.J. Chen, Mix proportions and mechanical properties of concrete containing very high-volume of Class F fly ash. Constr. Build. Mater., 46 (2013) 71–78. doi:doi.org/10.1016/j.conbuildmat.2013.04.016.

[34]- A. Sil, D.K.S. Roy, Performance of High Volume Fly Ash Concrete Using Local Power Plant Fly Ash. Int. J. Compos. Const. Mater., 1 (2015) 7-13.

[35]- R. Siddique, Performance characteristics of high-volume Class F fly ash concrete. Cem. Concr. Res., 34 (2004) 487-493. doi:doi.org/10.1016/j.cemconres.2003.09.002.

[36]- R.K. Majhi, A.N. Nayak, Properties of Concrete Incorporating Coal Fly Ash and Coal Bottom Ash. J. Inst. Eng. Ser. A., 100 (2019) 459-469. doi:doi.org/10.1007/s40030-019-00374-y.

[37]- N. Singh, P. Kumar, P. Goyal, Reviewing the behaviour of high volume fly ash based self compacting concrete. J. Build. Eng., 26 (2019) 100882. doi:doi.org/10.1016/j.jobe.2019.100882.

[38]- IS: 8112, ORDINARY PORTLAND CEMENT, 43 GRADE - SPECIFICATION, New Delhi. (2013).

[39]- ASTM C 618, Standard Specification for Coal Fly Ash and Raw or Calcined Natural Pozzolan for Use in Concrete. (2014). doi:doi.org/10.1520/C0618.

[40]- IS:383, Indian Standard Coarse and Fine aggregate for Concrete- Specification, B.I. Stand, Editor New Delhi, India. (2016). 1-21.

[41]- IS 9103, Specification for Concrete Admixtures, Bur. Indian Stand. Dehli. (1999). 1–22.
[42]- N. Su, K.C. Hsu, H.W. Chai, A simple mix design method for self-compacting concrete. Cem. Concr. Res., 31 (2001) 1799-1807. doi:doi.org/10.1016/S0008-8846(01)00566-X.
[43]- EFNARC, The European guidelines for self-compacting concrete specification, production and use. (2005).
[44]- IS 516, Hardened Concrete —Methods of Test, Part 1: Testing of Strength of Hardened Concrete, New Delhi, n.d.
[45]- IS 5816, Splitting tensile strength of concrete method of test, New Delhi. (1999).
[46]- IS 13311, Nondestructive testing of concrete- methods of test (Part 1), New Delhi. (1992).
[47]- ASTM C1585, Standard test method for measurement of rate of absorption of water by hydraulic cement concretes. (2004). doi:doi.org/10.1520/C1585-13.2.
[48]- AASHTO T 358, Standard Method of Test for Surface Resistivity Indication of Concrete's Ability to Resist Chloride Ion Penetration, Washington. (2022(accessed March 20, 2023).).
[49]- A.A. Kadir, M.I.H. Hassan, M.M.A.B. Abdullah, Investigation on Leaching Behaviour of Fly Ash and Bottom Ash Replacement in Self-Compacting Concrete. IOP Conf. Ser. Mater. Sci. Eng., 133 (2016). doi:doi.org/10.1088/1757-899X/133/1/012036.
[50]- M. Rafieizonooz, J. Mirza, M.R. Salim, M.W. Hussin, E. Khankhaje, Investigation of coal bottom ash and fly ash in concrete as replacement for sand and cement. Constr. Build. Mater., 116 (2016) 15-24. doi:doi.org/10.1016/j.conbuildmat.2016.04.080.
[51]- R. Martínez-García, I.M. Guerra-Romero, J.M. Morán-del Pozo, J. de Brito, A. Juan-Valdés, Recycling aggregates for self-compacting concrete production: A feasible option. Materials (Basel), 13 (2020) 1-19. doi:doi.org/10.3390/ma13040868.
[52]- M. Tuyan, A. Mardani-Aghabaglou, K. Ramyar, Freeze-thaw resistance, mechanical and transport properties of self-consolidating concrete incorporating coarse recycled concrete aggregate. Mater. Des., 53 (2014) 983–991. doi:doi.org/10.1016/j.matdes.2013.07.100.
[53]- V.M. Modani, P.O.Mohitkar, Self-compacting concrete with recycled aggregate: A solution for sustainable development. Int. J. Civ. Struct. Eng., 4 (2014) 430-440. doi:doi.org/https://doi.org/10.6088/ijcser.201304010041.
[54]- N. Singh, S.P. Singh, Carbonation and electrical resistance of self compacting concrete made with recycled concrete aggregates and metakaolin. Constr. Build. Mater., 121 (2016) 400-409. doi:doi.org/10.1016/j.conbuildmat.2016.06.009.
[55]- R. Kurda, J. de Brito, J.D. Silvestre, Influence of recycled aggregates and high contents of fly ash on concrete fresh properties. Cem. Concr. Compos. J., 84 (2017). doi:198–213.
[56]- M. Singh, R. Siddique, K. Ait-Mokhtar, R. Belarbi, Durability Properties of Concrete Made with High Volumes of Low-Calcium Coal Bottom Ash As a Replacement of Two Types of Sand. J. Mater. Civ. Eng, 28 (2015) 04015175. doi:doi.org/10.1061/(asce)mt.1943-5533.0001464.
[57]- I. Yüksel, T. Bilir, Ö. Özkan, Durability of concrete incorporating non-ground blast furnace slag and bottom ash as fine aggregate. Build. Environ., 42 (2007) 2651–2659. doi:doi.org/10.1016/j.buildenv.2006.07.003.
[58]- R.U.D. Nassar, N. Singh, S. Varsha, A.R. Sai, M. Sufyan-Ud-Din, Strength, electrical resistivity and sulfate attack resistance of blended mortars produced with agriculture waste ashes, Case Stud. Constr. Mater., 16 (2022) 1-16. doi:doi.org/10.1016/j.cscm.2022.e00944.
[59]- A. Simalti, A.P. Singh, Comparative study on performance of manufactured steel fiber and shredded tire recycled steel fiber reinforced self-consolidating concrete. Constr. Build. Mater., 266 (2021) 121102. doi:doi.org/10.1016/j.conbuildmat.2020.121102.
[60]- M. Mastali, A. Dalvand, Use of silica fume and recycled steel fibers in self-compacting concrete (SCC),. Constr. Build. Mater., 125 (2016) 196-209. doi:doi.org/10.1016/j.conbuildmat.2016.08.046.
[61]- B. Sukumar, Evaluation of strength at early ages of self-compacting concrete with high volume fly ash. J. const. build. mat., 22 (2008) 1394-1401. doi:doi.org/10.1016/j.conbuildmat.2007.04.005.
[62]- M. Sahmaran, I.O. Yaman, M. Tokyay, Transport and mechanical properties of self consolidating concrete with high volume fly ash. Cem. Concr. Compos. J., 31 (2009) 99-106. doi:doi.org/10.1016/j.cemconcomp.2008.12.003.